



Article

Spatial and Temporal Variation in Vegetation Cover and Its Response to Topography in the Selinco Region of the Qinghai-Tibet Plateau

Hongxin Huang [†], Guilin Xi [†] , Fangkun Ji, Yiyang Liu, Haoran Wang and Yaowen Xie ^{*}

College of Earth and Environmental Sciences, Lanzhou University, Lanzhou 730000, China; 220220947351@lzu.edu.cn (H.H.); xigl21@lzu.edu.cn (G.X.); 220220947371@lzu.edu.cn (F.J.); liuyy2021@lzu.edu.cn (Y.L.); wanghr2021@lzu.edu.cn (H.W.)

^{*} Correspondence: xieyw@lzu.edu.cn

[†] These authors contributed equally to this work.

Abstract: In recent years, the vegetation cover in the Selinco region of the Qinghai-Tibet Plateau has undergone significant changes due to the influence of global warming and intensified human activity. Consequently, comprehending the distribution and change patterns of vegetation in this area has become a crucial scientific concern. To address this concern, the present study employed MODIS-NDVI and elevation data, integrating methodologies such as trend analysis, Hurst exponent analysis, and sequential cluster analysis to explore vegetation cover changes over the past 21 years and predict future trends, while examining their correlation with topographic factors. The study findings indicate a fluctuating upward trend in vegetation cover, with a notable decrease in 2015. Spatially, the overall fractional vegetation cover (FVC) in the study area showed a basic stability with a percentage of 78%. The analysis of future trends in vegetation cover revealed that the majority of areas (68.26%) exhibited an uncertain trend, followed by stable regions at 15.78%. The proportion of areas showing an increase and decrease in vegetation cover accounted for only 9.63% and 5.61%, respectively. Elevation and slope significantly influence vegetation cover, with a trend of decreasing vegetation cover as elevation increases, followed by an increase, and then another decrease. Likewise, as the slope increases, initially, there is a rise in vegetation cover, followed by a subsequent decline. Notably, significant abrupt changes in vegetation cover are observed within the 4800 m elevation band and the 4° slope band in the Selinco region. Moreover, aspect has no significant effect on vegetation cover. These findings offer comprehensive insights into the spatial and temporal variations of vegetation cover in the Selinco region and their association with topographic factors, thus serving as a crucial reference for future research.

Keywords: fractional vegetation cover; spatial and temporal variation characteristics; trend analysis; Hurst exponent; topographic factor



Citation: Huang, H.; Xi, G.; Ji, F.; Liu, Y.; Wang, H.; Xie, Y. Spatial and Temporal Variation in Vegetation Cover and Its Response to Topography in the Selinco Region of the Qinghai-Tibet Plateau. *Remote Sens.* **2023**, *15*, 4101. <https://doi.org/10.3390/rs15164101>

Academic Editor: Liming Zhou

Received: 24 June 2023

Revised: 17 August 2023

Accepted: 18 August 2023

Published: 21 August 2023



Copyright: © 2023 by the authors. Licensee MDPI, Basel, Switzerland. This article is an open access article distributed under the terms and conditions of the Creative Commons Attribution (CC BY) license (<https://creativecommons.org/licenses/by/4.0/>).

1. Introduction

Vegetation is of great importance in physical geography and terrestrial ecosystems, as it plays a crucial role in multiple processes such as the hydrological cycle, surface energy exchange, climate change, geochemical cycles, and land cover change [1–4]. In recent years, the escalating trend of global warming has brought climate change to the forefront of scientific research [5]. The Qinghai-Tibet Plateau, as a highly vulnerable region to climate warming, has attracted significant attention from scholars worldwide [6,7]. Moreover, the region faces challenges due to frequent human activity, including overgrazing and indiscriminate logging, which have resulted in severe ecological and environmental problems such as grassland degradation, soil erosion, desertification, and biodiversity loss [8,9]. Thus, in light of global warming and the escalating ecological problems, conducting comprehensive research on vegetation change patterns and their influencing factors on the

Tibetan Plateau can contribute to the promotion of sustainable development and ecological conservation in the region.

Fractional vegetation cover (FVC) represents the proportion of an area covered by vegetation in relation to the total area of a specific region. It serves as a pivotal indicator for assessing vegetation distribution, coverage, and overall ecological health [10]. The calculation of FVC is commonly employed to evaluate the quality of the ecological environment, changes in land use and land cover, and the impacts of climate change on ecosystems [11–13]. Currently, there are two primary methods for calculating FVC: traditional ground measurements and remote sensing inversion [14,15]. Traditional ground measurement methods involve field sampling, visual estimation, photographic documentation, and instrumental monitoring [16,17]. However, these approaches exhibit notable drawbacks, including relatively low representativeness, diminished accuracy, and a considerable workload. As a consequence, remote sensing inversion emerges as the preferred method for practical monitoring applications. In recent years, numerous researchers have harnessed remote sensing techniques to infer FVC from satellite imagery and to analyze its spatial and temporal variations [11,18]. Nevertheless, FVC exhibits significant geographical disparities over time and space, attributable to variations in hydrothermal conditions and geographic environments across different study areas [19]. This means that FVC may be influenced by diverse factors in different regions, such as precipitation, temperature, and soil type. Therefore, it is essential to account for and rectify these geographical differences when studying FVC changes, ensuring the credibility and precision of the outcomes. Additionally, it is pivotal to conduct further investigations into the correlation between FVC and geographic as well as climatic factors to gain a more profound comprehension of its underlying mechanisms of change. Such exploration can provide a scientific foundation for ecological environmental protection and sustainable development.

The type and distribution of vegetation cover are intricately linked to the topography of an area. Variations in topography profoundly influence the hydrothermal conditions of the land surface and also exert a certain level of influence on the scope and character of human activity. Consequently, these factors directly or indirectly shape the spatial and temporal distribution patterns of vegetation cover [20,21]. Studies from other comparable locations have demonstrated the significant role of topographic factors in influencing vegetation cover. For instance, Huang et al. [22] observed a general pattern of increasing and then decreasing vegetation cover with elevation in the Qin Mountains region. Below an elevation of 3300 m, there was a noticeable increase in vegetation cover, particularly in farmland and grassland areas. Conversely, above 3300 m above sea level, forest cover prevailed, although with lower vegetation cover values. Similarly, Li et al. [23] noted a shift of low vegetation cover toward high slope areas and high vegetation cover toward low slope areas in the southern part of the Loess Plateau. Wang's study in the Three Parallel Rivers Region (TPRR) revealed that the proportion of vegetation cover was highest on semi-shady slopes (35.25%), followed by semi-sunny slopes, and lowest on sunny slopes (27.83%) [24]. Therefore, it is imperative to conduct further investigations into the changes in vegetation cover that occur when elevation, slope, and aspect change. This analysis will enable us to understand the temporal and spatial patterns of vegetation cover and identify their underlying causes.

The Selinco region serves as a crucial ecological barrier of the Qinghai-Tibet Plateau and encompasses key ecosystems with rich vegetation and fauna resources [9]. These ecosystems include alpine meadows, alpine steppes, grasslands, and pasture areas. They play a vital role in maintaining the ecological security and stability of the Qinghai-Tibet Plateau [25]. Furthermore, the Selinco region boasts significant human resources and a wealth of historical and cultural heritage, including religious, folk, and historical culture [26]. Given its distinctive natural environment and rich cultural background, the region has emerged as a significant hotspot for ecological and environmental research. In recent years, the vegetation cover in the Selinco region has experienced significant changes attributed to factors such as climate change, human activity, and natural disasters. Gao's

study revealed the severe degradation of vegetation cover in the Northern Tibet region, with degraded areas accounting for 50.8% of the total area in 2004, including 8.0% experiencing severe degradation and 1.7% experiencing very severe degradation. The grassland degradation index was particularly severe in the middle, eastern, and northern regions of Northern Tibet, while the degradation index for vegetation cover was relatively lower in the vast western region [27]. Additionally, Tahir et al. [28] observed an overall decreasing trend in vegetation cover in the Naqu River basin from 1982 to 2015, with variations in the dynamics of vegetation cover across different time periods.

Based on the current state of research in the Selinco region, there is a need for a topographic factor-based analysis of the spatial and temporal variation of vegetation cover in the region. This study will use MOD13Q1 remote sensing data from 2000 to 2020 and the dimidiate pixel model to quantitatively extract and classify the vegetation cover of the Selinco region. Secondly, we will use the linear trend analysis method as well as the Hurst exponent to explore the long-term trends of vegetation cover in the Selinco region as well as predicting future trends. We will also consider the influence of topographic factors and use sequential cluster analysis to classify the Selinco region into different topographic factor classification areas. We will analyze the differences in vegetation cover in different topographic regions and explore the mechanism of the influence of topographic factors on vegetation distribution. The specific research questions addressed in this study are as follows: (1) What are the trend signatures of vegetation cover changes over the past 21 years and in the future? (2) How do different topographic factors affect vegetation cover? Through these analyses, we will be able to grasp the patterns and influencing factors of vegetation cover changes more comprehensively and accurately. This will provide stronger support for future ecological environment protection and restoration, pastoralism development, and sustainable development of the Qinghai-Tibet Plateau.

2. Materials and Methods

2.1. Study Area

The Selinco region is located in the northern Qinghai-Tibet Plateau, ranging from 29°56′ to 36°28′N and 85°3′ to 93°1′E. It encompasses five counties and one district in the western part of the Naqu region of the Tibet Autonomous Region, namely, Nima County, Shuanghu County, Shenzha County, Bange County, Anduo County, and Seni District (Figure 1) [9]. Covering a total area of approximately 300,000 km², the region features rugged terrain and an altitude range of 4139 to 6941 m. The topography of the study area consists of a central lowland surrounded by higher elevations [29]. The climate in this region falls within the Plateau temperate and subarctic climate zones, characterized by intense radiation and prolonged sunshine, with annual average temperature for each county in the Selinco region ranging from 0.9 to 3.3 °C, and annual precipitation ranging between 100 and 200 mm [9]. Due to the elevated average altitude and undulating terrain, the region boasts a diverse array of vegetation, with the main vegetation types being alpine steppe, alpine meadow steppe, alpine meadow, and alpine desert steppe, accounting for 52.66%, 18.39%, 18.37%, and 10.56%, respectively [30]. However, plant production in this area is restricted due to the short annual growing season, which lasts only about 150 days (May–September) [30]. Consequently, plant ecosystems in this region must undergo rapid growth and reproduction during this brief period to adapt to the specific climatic conditions.

2.2. Data Sources and Processing

The Normalized Difference Vegetation Index (NDVI) data employed in this study were acquired from the MOD13Q1 product dataset provided by the Land Processes Distributed Active Archive Center (LP DAAC). Specifically, NDVI data from the MOD13Q1 dataset during the growing season (May–September) from 2000 to 2020 were chosen, with a spatial resolution of 250 m and a temporal resolution of 16 days, selecting the first and seventeenth day NDVI data. To mitigate the effects of clouds and atmospheric interference, monthly maximum NDVI values were synthesized for two data periods within each month using

the Google Earth Engine (GEE) platform. This synthesis allowed for the characterization of monthly NDVI values. This approach entailed selecting the image element with the highest NDVI value within each month to capture the most accurate vegetation signal and ensure data precision and consistency. Moreover, the monthly data were subsequently averaged annually to acquire reliable year-by-year NDVI data.

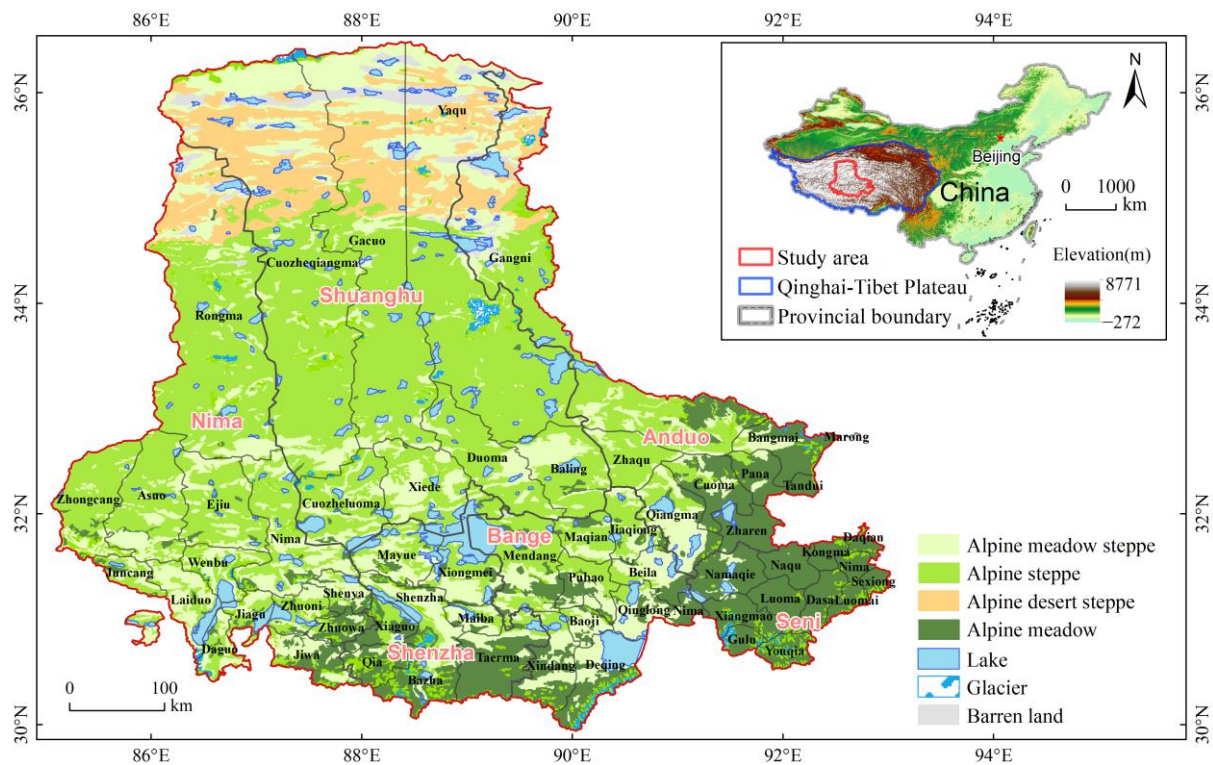


Figure 1. Geographical position and land cover map of the Selinco region (1:1 million vegetation type data were gained from the Resource Environment Science and Data Center, Chinese Academy of Sciences (<https://www.resdc.cn/>), accessed on 25 February 2023).

The digital elevation model (DEM) data utilized in this study were sourced from NASA and are accessible via NASA's website "<http://srtm.csi.cgiar.org/srtmdata/>" (accessed on 14 February 2023)". These DEM data possess a spatial resolution of 30 m, offering intricate topographic information. To further analyze the topographic characteristics of the study area, we employed ARCGIS software to extract data on key topographic factors such as elevation, slope, and aspect (Figure 2). Understanding these topographic factors is crucial for comprehending the relief and complexity of the study area's terrain. Subsequently, we adjusted the resolution of these topographic factors to 250 m to ensure consistency with the spatial resolution of the MODIS data used. By acquiring and analyzing the DEM data, we gained valuable insights into the topographic features of the study area and their correlation with vegetation growth. This correlation facilitates the elucidation of the driving mechanisms behind spatial and temporal changes in vegetation within the study area.

2.3. Research Methods

2.3.1. Vegetation Coverage

The dimidiate pixel model is a ground cover classification method that relies on remotely sensed image data [31]. It operates by classifying each image element, or pixel, in the remote sensing image as either vegetation or non-vegetation, thereby enabling the calculation of vegetation coverage [32]. Additionally, the dimidiate pixel model is

reproducible and can be applied at different times and locations to yield consistent results. The equation of the model is:

$$FVC = \frac{NDVI - NDVI_{soil}}{NDVI_{veg} - NDVI_{soil}} \quad (1)$$

where FVC represents the vegetation coverage, $NDVI_{soil}$ represents the $NDVI$ value of the area completely covered by bare soil or devoid of vegetation, and $NDVI_{veg}$ is the $NDVI$ value of the image element entirely covered by vegetation. In an ideal scenario, $NDVI_{veg}$ would be equivalent to $NDVI_{max}$ and $NDVI_{soil}$ would be equal to $NDVI_{min}$. However, there is unavoidable noise in the image; therefore, instead of using the maximum and minimum values of $NDVI$ in the area, a confidence interval of 5% to 95% is used for calculating the vegetation cover [33].

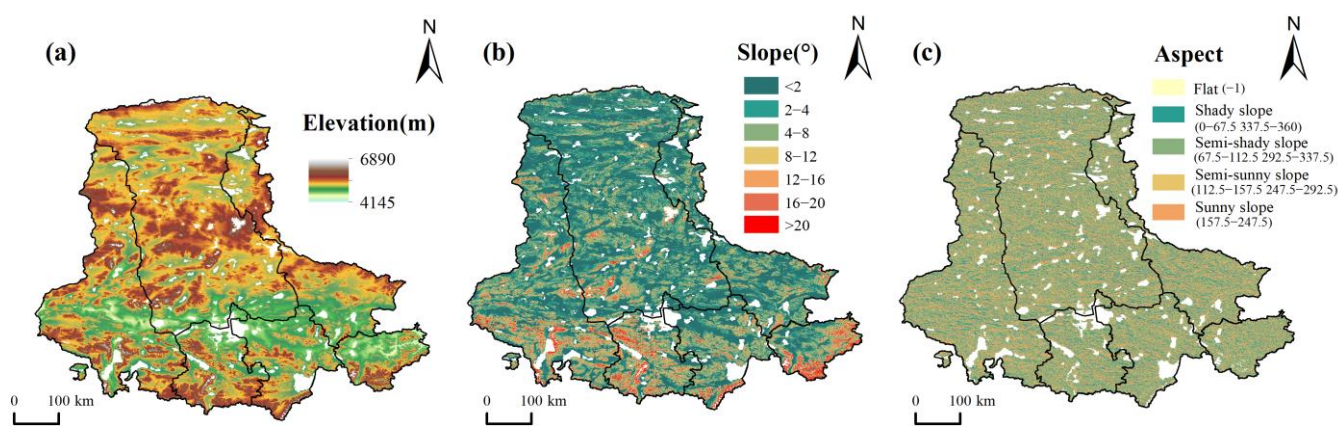


Figure 2. (a) Elevation distribution (b) slope distribution, and (c) aspect classification across the Selinco region.

2.3.2. Trend Analysis and Significance Test

In this study, we employed the trend analysis method to evaluate the trend of fraction of vegetation cover (FVC) values over an extended time series. The trend analysis method utilizes the least squares method to compute the slope for each image element, thereby elucidating the long-term trend of vegetation cover [34,35]. The slope calculation formula is provided below:

$$S_{FVC} = \frac{n \times \sum_{i=1}^n i \times FVC_i - \sum_{i=1}^n i \sum_{i=1}^n FVC_i}{n \times \sum_{i=1}^n i^2 - (\sum_{i=1}^n i)^2} \quad (2)$$

where S_{FVC} represents the slope of FVC in the study time period, FVC_i is the average value of FVC in year i , i corresponds to the specific years, and n represents the total study years ($n = 21$). A positive value of S_{FVC} (>0) indicated an increasing trend in vegetation cover for the corresponding image element, while a negative value of S_{FVC} (<0) indicated a decreasing trend. The significance of the calculated S_{FVC} images was assessed using an F-test. A p -value greater than 0.05 indicated a non-significant change, a p -value between 0.01 and 0.05 indicated a significant change, and a p -value less than 0.01 indicated a highly significant change. The level of significance served as an indicator of the reliability of the S_{FVC} images.

$$F = U \times \frac{n-2}{Q} \quad (3)$$

$$U = \sum_{i=1}^n (\hat{y}_i - \tilde{y})^2 \quad (4)$$

$$Q = \sum_{i=1}^n (y_i - \hat{y}_i)^2 \tag{5}$$

where U denotes the error sum of squares, Q denotes the regression sum of squares, y_i represents the *FVC* image element value in year i , \hat{y}_i denotes the regression value of *FVC* in year i , \tilde{y} denotes the mean value of *FVC* during the study period, and n denotes the number of years ($n = 21$). Comparing the F -values with the F -test table, the results were classified into five categories: highly significant increase ($q > 0, p < 0.01$), significant increase ($q > 0, 0.01 < p < 0.05$), basically stable ($p > 0.05$), significant decrease ($q < 0, 0.01 < p < 0.05$), and highly significant decrease ($q < 0, p < 0.01$).

2.3.3. Hurst Exponent Analysis

The Hurst exponent analysis, based on the extreme difference analysis (R/S), is a quantitative method used to describe the information dependence of a study object within a time series [36]. The fundamental principle is as follows: given a time-series $\{FVC_t\} (t = 1, 2, 3, \dots, n)$, where τ represents any positive integer, the mean series can be defined as follows:

$$\widetilde{FVC}_\tau = \frac{1}{\tau} \sum_{t=1}^{\tau} FVC_t, \tau = 1, 2, 3, \dots, n \tag{6}$$

$$X(t, \tau) = \sum_{t=1}^{\tau} (FVC_t - \widetilde{FVC}_\tau), 1 \leq t \leq \tau \tag{7}$$

$$R_\tau = \max X(t, \tau) - \min X(t, \tau), \tau = 1, 2, 3, \dots, n \tag{8}$$

$$S_\tau = \left[\frac{1}{\tau} \sum_{t=1}^{\tau} (FVC_t - \widetilde{FVC}_\tau)^2 \right]^{\frac{1}{2}}, \tau = 1, 2, 3, \dots, n \tag{9}$$

$$\frac{R_\tau}{S_\tau} = (\alpha\tau)^H \tag{10}$$

where $X(t, \tau)$ is the cumulative deviation, R_τ is the extreme deviation, S_τ is the standard deviation, and H is the Hurst exponent. The value of the Hurst index can be obtained by applying the least squares method in the double logarithmic coordinate system ($\ln \tau, \ln \frac{R_\tau}{S_\tau}$). When $0.5 < H < 1$, it indicates a persistent time series, implying that the future trend aligns with the past trend. The closer H is to 1, the stronger the persistence of the time series. Conversely, when $H = 0.5$, the time series is considered random, with no long-term correlation between future and past change trends. For $0 < H < 0.5$, the time series exhibits anti-persistence, where the future change trend opposes the past trend. The closer H is to 0, the stronger the anti-persistence [37]. By superimposing the S_{FVC} plot on the Hurst exponent plot, the vegetation’s future trend plot was obtained, as presented in Table 1.

Table 1. Classification of the *FVC* variation in the future.

S_{FVC}	Hurst		
	$H < 0.4$	$0.4 < H < 0.6$	$H > 0.6$
$S < -0.001$	Increase	Uncertain	Decrease
$-0.001 \leq S \leq 0.001$	Stable	Uncertain	Stable
$S > 0.001$	Decrease	Uncertain	Increase

2.3.4. Abrupt Point Detection and Significance Test

To enhance the analysis of the relationship between topographic factors and vegetation cover in the study area, we utilized the sequential cluster analysis method to identify abrupt points within the topographic factor data series. This method relies on the concept of relative sequence and cluster analysis to identify abrupt points by comparing the relative

positions and cluster distributions of data points. Its fundamental principle is to minimize the sum of squares of similar deviations of the same class [38,39]. For the sequences x_1, x_2, \dots, x_n .

$$S = \min_{2 \leq \tau \leq n-1} \left\{ S_n(\tau) = \min_{2 \leq \tau \leq n-1} \left(\sum_{i=1}^{\tau} (x_i - \tilde{x}_{\tau})^2 + \sum_{i=\tau+1}^n (x_i - \tilde{x}_{n-\tau})^2 \right) \right\} \quad (11)$$

where $\tilde{x}_{\tau} = \frac{1}{\tau} \sum_{i=1}^{\tau} x_i$, $\tilde{x}_{n-\tau} = \frac{1}{n-\tau} \sum_{i=\tau+1}^n x_i$ are the means of the two parts before and after τ , respectively, and when S is minimal, the corresponding τ is the optimal splitting point, i.e., τ is the abrupt change point. The rank-sum test can be used to test the significance of the abrupt point [40,41]. For a given abrupt point τ , the sequence x_i is divided into two sample sequences, n_1 and n_2 , where n_1 corresponds to the subsample size with fewer samples and n_2 corresponds to the subsample size with more samples. The statistic of U is computed as follows:

$$U = \frac{W - n_1(n_1 + n_2 + 1)/2}{\sqrt{n_1 n_2 (n_1 + n_2 + 1)/12}} \quad (12)$$

where W is the sum of the ranks of the smaller samples, U obeys the standard normal distribution, and the abrupt point is significant if $|U| > 1.96$.

3. Results

3.1. Characteristics of Vegetation Cover Change

3.1.1. Temporal Variation Characteristics

Figure 3 illustrates the inter-annual variation trend of the multi-year average fractional vegetation coverage (FVC) during the vegetation growing season in the Selinco region from 2000 to 2020. Overall, the annual average FVC of vegetation cover in the Selinco region shows a fluctuating upward trend, with a notable decrease in 2015. The overall growth rate is 0.004/10a (rate of change per decade). The multi-year average FVC during the vegetation growing season in the region has a relatively low value of 0.2171. The highest FVC value occurred in 2018, reaching 0.2415, while the lowest value was observed in 2015, with a value of 0.1822. These findings indicate that the vegetation cover condition in the Selinco region is generally low. Further analysis of the year-to-year changes in vegetation cover reveals that from 2000 to 2012, there was an overall fluctuating upward trend, with peaks in 2004 and 2012, reaching 0.2236 and 0.2254, and growth rates of 0.019/10a and 0.008/10a, respectively. However, from 2012 to 2015, the vegetation cover started to decline at a rate of $-0.118/10a$. Between 2015 and 2018, there was an increasing trend in vegetation cover, with a growth rate of 0.193/10a. In summary, the vegetation cover in the Selinco region has fluctuated over the past two decades. Although there is an overall increasing trend, significant inter-annual variations are observed. Particularly, the decreasing trend between 2012 and 2015 suggests the presence of influencing factors contributing to the decline in vegetation cover in the region. Further investigation of the causes and influencing factors of these changes will enhance our understanding of the vegetation dynamics in the Selinco region and provide a scientific basis for the ecological environment protection and management of the area.

3.1.2. Spatial Variation Characteristics

Figure 4 illustrates FVC values across various counties and the spatial distribution pattern of vegetation cover in the Selinco region. The multi-year annual average FVC values in Selinco exhibit a decreasing trend from south to north and an increasing distribution pattern from west to east. Among the counties, Seni District ranks highest in vegetation cover (0.5683), followed by Bange County (0.3202), Shenzha County (0.2971), Anduo County (0.2744), Nima County (0.1786), and Shuanghu County (0.1352). The southeastern region of Selinco exhibits the highest multi-year average FVC values, surpassing 0.5, and is primarily concentrated in Seni District and the southeastern part of Anduo County. Conversely,

the northern region demonstrates the lowest multi-year average FVC values, below 0.1, spanning the northern areas of Nima County, Shuanghu County, and Anduo County. This discrepancy can be attributed to the higher altitude prevailing in the northern portion of the study area.

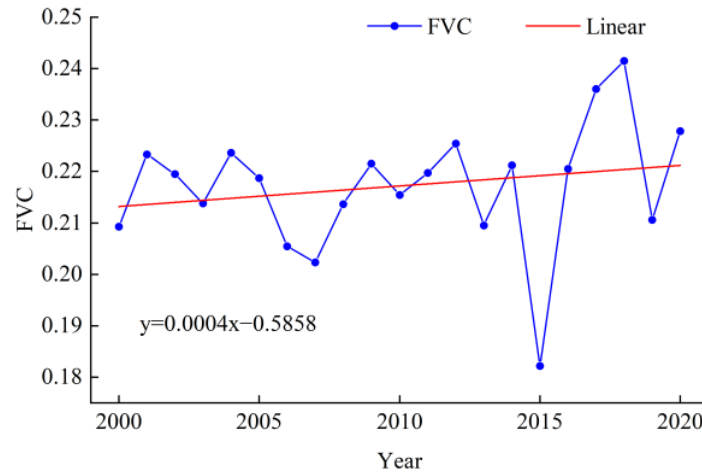


Figure 3. Trend in vegetation cover over time in the Selinco region during the growing season.

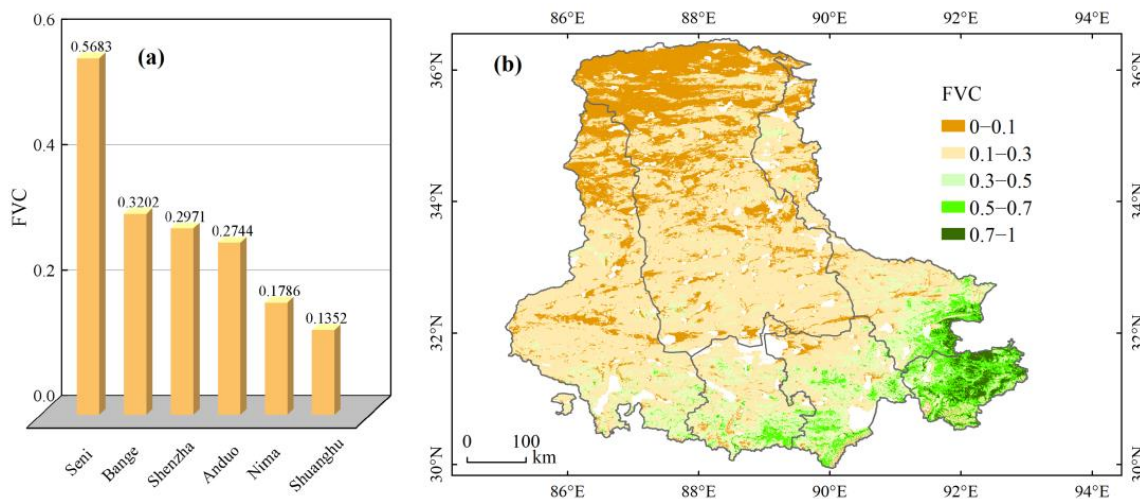


Figure 4. (a) FVC values for different counties and (b) spatial distribution of vegetation cover in the Selinco region during the growing season.

The inter-annual trend of FVC in the Selinco region from 2000 to 2020 is presented in Figure 5. The FVC demonstrates a predominantly stable trend, accounting for 77.68% of the region. An increasing trend is observed in 19% of the FVC, primarily in the northern areas of Shuanghu County and Anduo County, with 11.08% of the region exhibiting a highly significant increase and 7.92% exhibiting a significant increase. However, a decreasing trend is observed in 3.33% of the FVC, mainly in the southern areas of Shuanghu County and at the junction of Nima County, Shenzha County, and Bange County. Among these areas, 2.14% demonstrate a highly significant decrease and 1.19% show a significant decrease. It is worth noting that the increasing trend of FVC in the northern part of the study area surpasses that of the southern part. This disparity may be attributed to the lower vegetation cover baseline in the southern region, leading to a more rapid growth rate in the northern region.

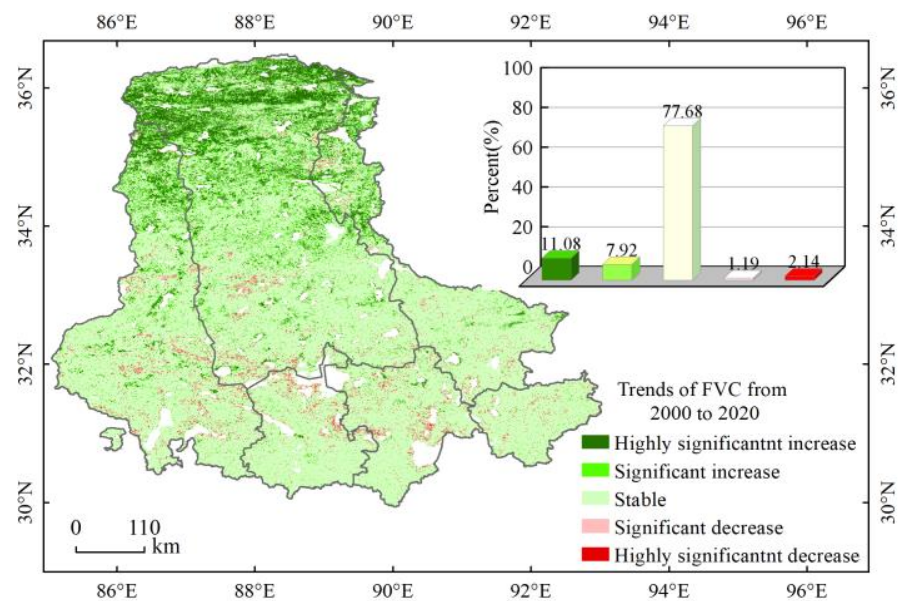


Figure 5. Trends in vegetation cover in the Selinco region during the growing season.

3.1.3. Future Change Trends

The distribution of areas in the Selinco region based on different Hurst exponent (H) levels is presented in Figure 6a. The average Hurst exponent (H) of the Selinco fraction of vegetation cover (FVC) was found to be 0.4491, ranging from 0.0848 to 0.9019. The proportion of pixels with $H < 0.5$ accounted for 72.8%, while only 27.2% of pixels had $H > 0.5$. These findings suggest that the future trend in most areas of Selinco contradicts the past trend, likely due to a slowdown in vegetation growth over the past decade. Notably, the range of H values between 0.4 and 0.6 exhibited the highest frequency, representing 69% of the image elements. This indicates a significant level of uncertainty in FVC changes within the Selinco region. Additionally, 27.83% of the image elements demonstrated strong inverse persistence ($H < 0.4$), while 3.17% exhibited strong persistence ($H > 0.6$). To enhance the analysis of future vegetation cover trends in the Selinco region, we superimposed the S_{FVC} derived from the trend analysis method on the Hurst exponent (H). This integration enabled us to generate a future vegetation cover change trend map, as depicted in Figure 6b. The analysis reveals that the overall trend of future vegetation cover change in the entire study area is characterized by uncertainty, accounting for 69% of the region. Approximately 15.8% of the vegetation remains stable, primarily concentrated in the northwestern part of the study area, specifically in Nima and Shuanghu Counties. Areas indicating future growth constitute 5.6% of the region and are scattered across the southern part of Seni District, Bange County, Anduo County, and Nima County. In contrast, the northern portion of Shuanghu County, Nima County, and Anduo County exhibits a future trend of vegetation cover degradation, representing 9.6% of the region.

In general, the projected expansion of vegetation in the entire Selinco region is overshadowed by the extent of degradation, and a significant proportion of uncertainty regarding future vegetation changes exists within the study area. Of particular concern is the substantial percentage (45.19%) of pixels exhibiting a Hurst exponent ranging from 0.4 to 0.5. This exponent suggests a contrasting future trend compared with the past. When considering the overall upward trajectory of vegetation over the past 21 years, it is plausible to assume a potential risk of degradation in future vegetation dynamics. Consequently, this issue warrants careful attention.

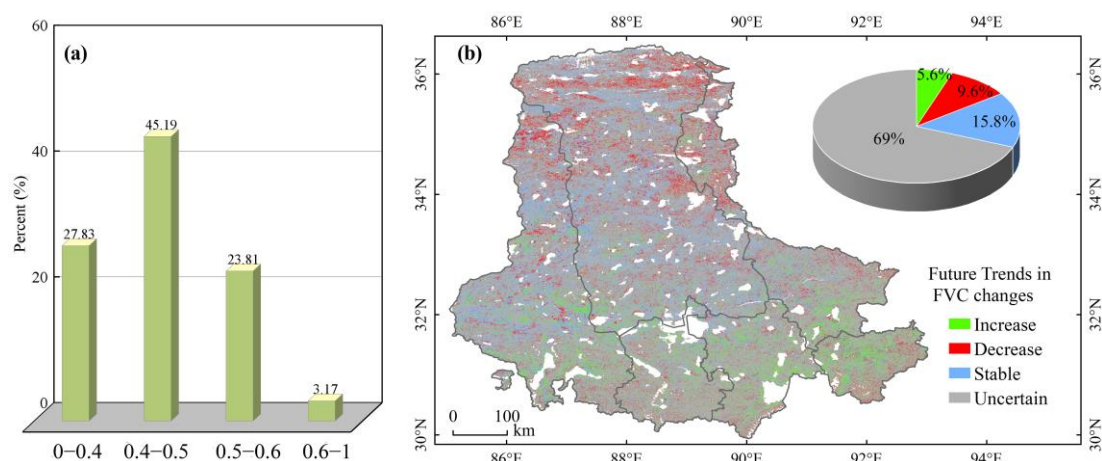


Figure 6. (a) The proportion of areas at different Hurst exponent levels and (b) spatial distribution of future vegetation trends in the Selinco region.

3.2. Relationship between Vegetation Cover Change and Different Topographic Factors

3.2.1. Analysis of the Response to Elevation

To investigate the relationship between vegetation cover change and elevation, we classified the Digital Elevation Model (DEM) data of the study area into 24 bands with a 50 m interval. We then superimposed these data on the annual average vegetation cover data spanning from 2000 to 2020 for in-depth analysis, enabling us to examine variations in vegetation cover across distinct elevation bands. Moreover, sequential cluster analysis was employed to derive vegetation cover variations and identify abrupt change patterns within each elevation band (Figure 7). The figure unequivocally illustrates that as altitude increases, the average FVC in the Selinco region manifests a general trend characterized by an initial decrease, a subsequent rise, and a final decrease. Particularly noteworthy are two elevation bands with abrupt changes, occurring at altitudes of 4800 m and 5450 m above sea level. Through the rank-sum test, we determined that the elevation band at 4800 m exhibited a significant change, while the band at 5450 m did not. Despite the insignificance of the abrupt change at 5450 m, considering the actual conditions in the study area, vegetation cover remained lower in elevation bands above 5450 m. Specifically, the area with elevations below 4800 m exhibited the highest vegetation cover, with an average of 0.2632, and its vegetation cover showed a non-significant decreasing trend at a rate of $-0.0026/50$ m. In the 4800–5450 m elevation range, the average vegetation cover was 0.2074, demonstrating a non-significant decreasing trend at a rate of $-0.0002/50$ m. In contrast, the area above 5450 m had the lowest vegetation cover with a mean value of 0.1376. Here, the vegetation cover exhibited a significant decreasing trend at a rate of $-0.0264/50$ m ($p < 0.05$), with the greatest variation (Std of 0.0309). The abrupt vegetation cover changes at 4800 m and 5450 m may be attributed to the type and distribution of vegetation. Alpine meadows were predominantly found in areas above 5450 m, while areas below 4800 m mainly consisted of alpine meadow steppe and alpine steppe. The 4800–5450 m region contained alpine desert steppe and alpine steppe (Table 2).

3.2.2. Response Analysis to Slope

To explore the correlation between vegetation cover change and slope, we divided the slope into 25 bands at 1° intervals, with slopes greater than 24° grouped into 25° bands. Subsequently, we overlaid these data with the annual average vegetation cover from 2000 to 2020 to analyze vegetation cover variations across different slope bands. Further, the sequential cluster analysis method was used to obtain the vegetation cover change and abrupt change graphs for each slope zone, as shown in Figure 8. It can be seen that as the slope increases, the average FVC of the Selinco region initially rises and then declines. Notably, the 4° band exhibits an abrupt change. A rank-sum test confirmed its statistical

significance at the $\alpha = 0.05$ level, thus indicating that 4° serves as a significant abrupt change point. Based on the above results, this study categorized the study area into two parts based on variations in slope, as outlined in Table 3. The first part corresponds to areas with slopes less than 4° , exhibiting low vegetation cover (mean value of 0.1916) and a highly significant increasing trend of vegetation cover at a rate of $0.0181/1^\circ$ ($p < 0.01$). The second part encompasses areas with slopes greater than 4° , characterized by relatively high vegetation cover (mean value of 0.2557) and a non-significant decreasing trend of vegetation cover at a rate of $-0.0008/1^\circ$. Additionally, the magnitude of vegetation cover change within this region was small (Std of 0.0156). Furthermore, no notable spatial distribution heterogeneity was observed among individual vegetation types across different slope zones (Table 3). Hence, the abrupt change in vegetation cover within the 4° region could potentially be attributed to the heightened human activity occurring in the lower slope region.

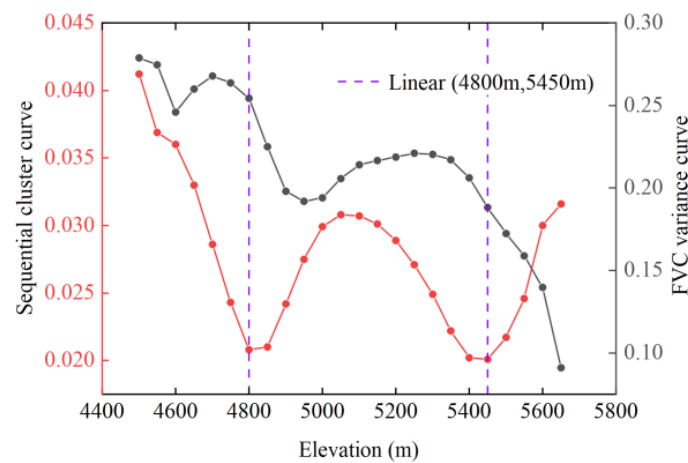


Figure 7. Vegetation cover change and abrupt change identification in each elevation zone.

Table 2. The characteristics of FVC values at different elevations.

Elevation Zone	Area (%)	Mean FVC	Slope (/50 m)	Std	Vegetation Type
<4800 m	21.49	0.2632	-0.0026	0.0105	Alpine meadow steppe; Alpine steppe
4800–5450 m	75.28	0.2074	-0.0002	0.0119	Alpine steppe; Alpine desert steppe
>5450 m	3.23	0.1376	-0.0264	0.0309	Alpine meadow

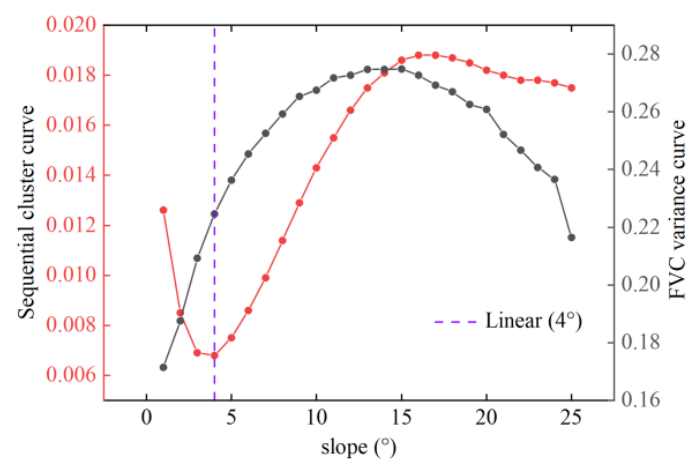


Figure 8. Vegetation cover change and abrupt change identification in each slope zone.

Table 3. The characteristics of FVC values at different slopes.

Slope Zone	Area (%)	Mean FVC	Slope (1°)	Std	Vegetation Type
<4°	60.12	0.1916	0.0181	0.0203	Alpine steppe; Alpine desert steppe;
>4°	39.88	0.2557	−0.0008	0.0156	Alpine meadow; Alpine meadow steppe

3.2.3. Response Analysis to Aspect

In order to investigate the relationship between vegetation change and aspect, we classified the aspect as shady slopes (0–67.5, 337.5–360), semi-shady slopes (67.5–112.5, 292.5–337.5), semi-sunny slopes (112.5–157.5, 247.5–292.5), and sunny slopes (157.5–247.5), and then superimposed these on the annual average vegetation cover from 2000 to 2020. The results are shown in Table 4. The results indicate that the vegetation cover on shady slopes is slightly higher than on sunny slopes. The order of vegetation cover for each aspect is as follows: semi-shady slopes (0.2238), shady slopes (0.2208), semi-sunny slopes (0.2206), and sunny slopes (0.2116). The differences in vegetation cover among the aspects are small, with the maximum difference being 1.22%. Upon further exploration of the vegetation cover of each aspect at different elevations and slopes, it was found that the maximum difference in the vegetation cover of each aspect across the range of elevations and slopes was 1.24% (4800–5450 m) and 1.81% (>4°). This was much lower than the maximum difference in the vegetation cover due to the different elevations or slopes, which were 12.56% and 6.41%, respectively. In addition, vegetation cover was greater on sunny slopes than on shady slopes at elevations greater than 5450 m. These findings suggest that aspect has no significant effect on vegetation cover in the Selinco region.

Table 4. The characteristics of FVC values at different elevations, slopes, and aspects.

Aspect Zone	Mean FVC	Elevation (m)			Slope (°)	
		<4800	4800–5450	>5450	<4	>4
shady slopes	0.2208	0.2711	0.2101	0.1419	0.1934	0.2604
semi-shady slopes	0.2238	0.2682	0.2136	0.1511	0.1971	0.2657
semi-sunny slopes	0.2206	0.2648	0.2103	0.1499	0.1951	0.2608
sunny slopes	0.2116	0.2591	0.2012	0.1461	0.1871	0.2476
Maximum minus minimum	0.0122	0.012	0.0124	0.0092	0.01	0.0181

4. Discussion

4.1. Analysis of Vegetation Cover Changes

This study employs MODIS-NDVI data to analyze the spatial and temporal variations in vegetation cover in the Selinco region over the past 21 years, along with its correlation with topographic factors. The findings demonstrate a fluctuating increasing trend in vegetation cover in the Selinco region over the last two decades, which aligns with previous research conducted by Jiao et al. [19]. Since the 1850s, the Qinghai-Tibet Plateau has experienced significant warming, with a warming rate approximately twice that of global warming [42], and precipitation has exhibited a non-significant increasing trend [43], indicating a period of warming and wetting on the plateau in recent years. Furthermore, ecological restoration initiatives, such as grazing bans, grassland restoration, and compensation for ecological protection, have been implemented on the Qinghai-Tibet Plateau since 2004 [44], exerting a positive influence on vegetation growth [45,46]. Most studies now attribute long-term changes in vegetation cover to climate change, while recognizing human activity as significant drivers of short-term variations [47,48]. Thus, in the Selinco region, the increase in vegetation cover can be attributed to a combination of factors, including a warming climate, increased precipitation, reduced livestock, and the establishment of ecological reserves. However, during the vegetation growing season of 2015, the FVC values exhibited a significant downward trend. This decline is likely

related to the occurrence of the super El Niño event in 2015/2016, which resulted in a substantial decrease in precipitation in the Selinco region. In fact, certain weather stations recorded precipitation levels that were over 35% lower than those typically observed in normal years [49,50]. In conclusion, the vegetation cover in the study area has shown a fluctuating upward trend over the past 21 years, influenced by both climate change and human activity. This trend may also impact future vegetation cover to some extent. However, apart from climate change and human activity, other factors such as solar radiation [51], winter snow [52], and permafrost soil [6,53] could also significantly affect the growth and distribution of vegetation in the Selinco region. Therefore, it is crucial for future studies to take into account the influence of multiple factors on vegetation cover in order to ensure the reliability of the results.

The average Hurst exponent was calculated based on the FVC data of the Selinco region, resulting in a value of 0.4491. Approximately 68.23% of the pixels exhibited a Hurst exponent ranging from 0.4 to 0.6, suggesting significant uncertainty in future vegetation changes in the Selinco region, consistent with Chen's findings [54]. The Hurst exponent, which relies on the long-term correlation of time-series data, serves as an effective method to predict potential future change trends. Its calculation primarily relies on the FVC data spanning 2000 to 2020. Analyzing this FVC data over the past 21 years uncovered a significant decline between 2012 and 2015. This disruption of the previous pattern of continuous FVC growth since 2010 introduces uncertainty in projecting future vegetation cover changes. It is crucial to acknowledge that the Hurst exponent focuses solely on the calculation of time-series FVC data, without considering other influential factors such as climate change and human activity. Since climate and human activity exhibit temporal variations, these factors should be taken into consideration when predicting future vegetation cover changes in the Selinco region. Furthermore, the Hurst exponent does not precisely estimate the duration of vegetation change and therefore entails a certain degree of uncertainty. Consequently, the development of corresponding measures requires thorough consideration of the possibility of vegetation degradation and persistence, along with further research to enhance the accuracy of predictions [55].

4.2. Analysis of Vegetation Cover Variations with Topography

Significant differences in vegetation cover were observed across various topographic environments within the study area. More precisely, the growing season FVC was significantly lower in high elevation areas compared with other zones. Furthermore, overall vegetation cover exhibited a decreasing trend with increasing elevation, which is consistent with the findings of some scholars [56,57]. Moreover, as slope increased, the growing season FVC showed an initial increase followed by a decrease, reaching its highest value at a slope of 15°. This finding aligns with Wang's study, with only a slight variation, wherein the maximum vegetation cover in the Three Parallel Rivers Region occurs at 35° [24]. These differences can be attributed to several factors. High-altitude regions experience reduced precipitation, prolonged exposure of surfaces to sunlight, and increased evaporation rates, leading to a gradual decline in soil moisture. Consequently, normal vegetation growth and development are hindered [58]. Furthermore, lower temperatures at higher altitudes reach the minimum threshold for vegetation growth, resulting in reduced vegetation cover [51,59]. Areas with gentle slopes experience higher levels of human activity, including overgrazing and indiscriminate logging. Consequently, these activities result in lower vegetation cover in areas with favorable water and heat conditions. However, as the slope increases, human intervention decreases, leading to a gradual recovery of vegetation cover toward the normal trend [60]. However, the intensity of human activity, vegetation types, and hydrothermal conditions vary across different areas. As a result, the locations of maximum vegetation cover may differ within the respective slope areas. Lastly, we discovered that aspect had minimal impact on vegetation cover in the Selinco region. This finding aligns with conclusions drawn from studies conducted in the Qingzhen Township of the Golog Tibetan Autonomous Prefecture [61] and the Ibiúna Plateau [62]. It is essential to note that

at high altitudes, a distinct altitudinal gradient exists, leading to varying climatic and environmental conditions. As altitude increases, temperatures decrease, and climatic conditions become harsher, imposing significant limitations on vegetation growth [63]. Therefore, changes in aspect do not cause dramatic shifts in vegetation cover at high altitudes; instead, elevation differences may be the primary contributing factor to changes in vegetation cover.

Therefore, when implementing ecological environmental protection initiatives, it is crucial to zone the Selinco region according to its diverse topographic conditions and implement appropriate protection policies. For instance, establishing alpine meadow protection zones is essential for high-altitude areas dominated by alpine meadows [64], where measures such as returning pasture to grass and controlling grazing can be employed to improve the survival rate of high-altitude vegetation [65]. In regions with lower slopes, efforts should focus on strengthening ecological construction projects such as artificial grass planting [66] and implementing sustainable grazing practices [67]. It is also vital to enhance the local population's awareness of ecological environmental protection to mitigate the negative impact of human activity on vegetation cover. In summary, the development of ecological environmental protection policies in the Selinco region should be tailored to local conditions, considering the distinct elevation gradient, slope distribution, and vegetation characteristics. Implementing different protection strategies based on these factors will contribute to restoring and enhancing the ecological environment of the Selinco region. This will provide strategic support for vegetation growth and the sustainable development of animal husbandry in the Qinghai-Tibet Plateau region.

4.3. Shortcomings and Prospects

The present study utilized an extensive time series of MODIS-NDVI remote sensing data to conduct a comprehensive and meticulous analysis of the spatiotemporal characteristics of vegetation cover in the Selinco region. Additionally, we conducted a meticulous investigation of the intricate correlations between these spatiotemporal attributes and topographic factors. Nevertheless, it is crucial to emphasize that despite the thoroughness of our study, certain limitations exist. A pivotal limitation stems from the data source. Our analysis solely relied on MODIS-NDVI and DEM data covering the period from 2000 to 2020. This dataset omits essential environmental variables such as temperature and precipitation data. Consequently, it was not possible to conduct an all-encompassing quantitative analysis that could unveil the intricate drivers behind vegetation cover variations. Furthermore, the lack of an inclusive and comparative assessment of diverse influences contributed to our inability to precisely identify the pivotal factors that exert a profound influence on the variations of vegetation cover. Although our analysis thoroughly investigated the interrelationships between vegetation cover and topographical characteristics (such as elevation and slope) in the Selinco region, effectively revealing abrupt transitional points and defining various regions of fluctuation, it was not possible to delve deeply into the fundamental triggers underpinning the significant shifts in vegetation cover within the Selinco region. This underscores the need for additional research efforts and dedicated attention to enhance our understanding of the mechanisms and determinants that drive these transformative variations. In conclusion, we recommend that future investigations should incorporate a wider spectrum of factors to attain a more holistic understanding of how topography influences the transformation of vegetation cover. For example, variables encompassing the distribution of unique vegetation types, shifts in land utilization, and geological characteristics should be taken into consideration. Such a comprehensive approach in future studies will provide heightened precision and more profound insights to significantly support ecological investigation and preservation endeavors.

5. Conclusions

This study utilized MODIS-NDVI data and DEM data from 2000 to 2020 to analyze the spatiotemporal variations of fractional vegetation cover (FVC) and its correlation with topographic factors (elevation, slope, and aspect) in the Selinco region over the past 21 years.

The analysis techniques employed included trend analysis, Hurst exponent analysis, and sequential cluster analysis. The findings demonstrate a general increasing trend in FVC across the Selinco region during the 21-year period, with a growth rate of 0.004 per decade. Nonetheless, a notable decline in FVC was observed in 2015. Regarding spatial variation, the vegetation cover across the study area exhibited a relatively consistent level of approximately 78%. An increasing trend was evident in 19% of the region, while a declining trend was noticeable in just 3%. The Hurst exponent analysis revealed an indistinct trend in future vegetation cover changes, accounting for 68.26% of the total areas studied. Approximately 5.61% of the areas were expected to maintain growth, scattered across the southern part of Seni District, Bange County, Anduo County, and Nima County. In contrast, the northern portion of Shuanghu County, Nima County, and Anduo County showed a degradation trend in vegetation cover, accounting for 9.63%. This implies a heightened vulnerability to vegetation cover deterioration in the Selinco region, underscoring the need for implementing measures to safeguard the region's ecological environment. Furthermore, our study revealed that elevation and slope exerted a substantial influence over vegetation cover, whereas aspect exerted a relatively minor effect. This is evident in the observed pattern of vegetation cover diminishing with rising elevation, succeeded by an upturn, and subsequently followed by a decline. Similarly, the augmentation of slope correlates with an initial increase and subsequent reduction in vegetation cover. The sequential cluster analysis highlighted significant abrupt changes in vegetation cover within the 4800 m elevation band and the 4° slope band in Selinco region. In summary, this study sought to clarify the spatiotemporal fluctuations in vegetation cover in the Selinco region, with a particular emphasis on investigating vegetation cover changes in relation to variations in topographic factors. This endeavor offers a valuable reference framework for future research pursuits.

Author Contributions: Methodology, H.H.; Validation, H.H. and G.X.; Formal analysis, H.H.; Investigation, H.H.; Resources, H.H.; Data curation, H.H.; Writing—original draft, H.H.; Writing—review and editing, G.X., F.J., Y.L. and H.W.; Visualization, G.X.; Supervision, G.X.; Project administration, Y.X.; Funding acquisition, Y.X. All authors have read and agreed to the published version of the manuscript.

Funding: We gratefully acknowledge the support provided by the Second Tibetan Plateau Scientific Expedition and Research Program (STEP) [2019QZKK0603], the National Key Research and Development Program of China [2018YFA0606404-03], and the Strategic Priority Research Program of the Chinese Academy of Sciences, Pan-Third Pole Environment Study for a Green Silk Road (Pan-TPE) [XDA2009000001].

Data Availability Statement: The MODIS-NDVI data are available from <https://lpdaac.usgs.gov> (accessed on 3 February 2023). The elevation data are available from <http://srtm.csi.cgiar.org/srtmdata> (accessed on 14 February 2023). The vegetation type data are available from <https://www.resdc.cn> (accessed on 25 February 2023). The data generated in this study can be obtained from the corresponding author.

Conflicts of Interest: The authors declare no conflict of interest.

References

1. Gao, L.; Wang, X.; Johnson, B.A.; Tian, Q.; Wang, Y.; Verrelst, J.; Mu, X.; Gu, X. Remote sensing algorithms for estimation of fractional vegetation cover using pure vegetation index values: A review. *ISPRS J. Photogramm. Remote Sens.* **2020**, *159*, 364–377. [[CrossRef](#)] [[PubMed](#)]
2. Wei, X.; Li, Q.; Zhang, M.; Giles-Hansen, K.; Liu, W.; Fan, H.; Wang, Y.; Zhou, G.; Piao, S.; Liu, S. Vegetation cover—Another dominant factor in determining global water resources in forested regions. *Glob. Chang. Biol.* **2018**, *24*, 786–795. [[CrossRef](#)] [[PubMed](#)]
3. Genxu, W.; Guangsheng, L.; Chunjie, L.; Yan, Y. The variability of soil thermal and hydrological dynamics with vegetation cover in a permafrost region. *Agric. For. Meteorol.* **2012**, *162–163*, 44–57. [[CrossRef](#)]
4. Yin, H.; Pflugmacher, D.; Li, A.; Li, Z.; Hostert, P. Land use and land cover change in Inner Mongolia—Understanding the effects of China's re-vegetation programs. *Remote Sens. Environ.* **2018**, *204*, 918–930. [[CrossRef](#)]

5. Huang, J.; Li, Y.; Fu, C.; Chen, F.; Fu, Q.; Dai, A.; Shinoda, M.; Ma, Z.; Guo, W.; Li, Z. Dryland climate change: Recent progress and challenges. *Rev. Geophys.* **2017**, *55*, 719–778. [[CrossRef](#)]
6. Cheng, G.; Wu, T. Responses of permafrost to climate change and their environmental significance, Qinghai-Tibet Plateau. *J. Geophys. Res. Earth Surf.* **2007**, *112*, 2156–2202. [[CrossRef](#)]
7. Chen, B.; Zhang, X.; Tao, J.; Wu, J.; Wang, J.; Shi, P.; Zhang, Y.; Yu, C. The impact of climate change and anthropogenic activities on alpine grassland over the Qinghai-Tibet Plateau. *Agric. For. Meteorol.* **2014**, *189–190*, 11–18. [[CrossRef](#)]
8. Li, X.; Gao, J.; Zhang, J.; Sun, H. Natural and anthropogenic influences on the spatiotemporal change of degraded meadows in southern Qinghai Province, West China: 1976–2015. *Appl. Geogr.* **2018**, *97*, 176–183. [[CrossRef](#)]
9. Xi, G.; Ma, C.; Xie, Y.; Guo, Z.; Bao, T.; Zhang, X.; Liu, Y.; Wang, H. Spatialization method of monitoring grazing intensity: A case-study of the Tibet Selinco basin, Qinghai-Tibet Plateau. *Land Degrad. Dev.* **2023**, *34*, 1311–1322. [[CrossRef](#)]
10. Purevdorj, T.S.; Tateishi, R.; Ishiyama, T.; Honda, Y. Relationships between percent vegetation cover and vegetation indices. *Int. J. Remote Sens.* **1998**, *19*, 3519–3535. [[CrossRef](#)]
11. Zhang, X.; Liao, C.; Li, J.; Sun, Q. Fractional vegetation cover estimation in arid and semi-arid environments using HJ-1 satellite hyperspectral data. *Int. J. Appl. Earth Obs. Geoinf.* **2013**, *21*, 506–512. [[CrossRef](#)]
12. Li, J.; Wang, J.; Zhang, J.; Liu, C.; He, S.; Liu, L. Growing-season vegetation coverage patterns and driving factors in the China-Myanmar Economic Corridor based on Google Earth Engine and geographic detector. *Ecol. Indic.* **2022**, *136*, 108620. [[CrossRef](#)]
13. Cai, Y.; Zhang, F.; Duan, P.; Jim, C.Y.; Chan, N.W.; Shi, J.; Liu, C.; Wang, J.; Bahtebay, J.; Ma, X. Vegetation cover changes in China induced by ecological restoration-protection projects and land-use changes from 2000 to 2020. *Catena* **2022**, *217*, 106530. [[CrossRef](#)]
14. Zhou, Q.; Robson, M. Automated rangeland vegetation cover and density estimation using ground digital images and a spectral-contextual classifier. *Int. J. Remote Sens.* **2001**, *22*, 3457–3470. [[CrossRef](#)]
15. Lü, L.; Zhao, Y.; Chu, L.; Wang, Y.; Zhou, Q. Grassland coverage change and its humanity effect factors quantitative assessment in Zhejiang province, China, 1980–2018. *Sci. Rep.* **2022**, *12*, 18288. [[CrossRef](#)] [[PubMed](#)]
16. White, M.A.; Asner, G.P.; Nemani, R.R.; Privette, J.L.; Running, S.W. Measuring Fractional Cover and Leaf Area Index in Arid Ecosystems: Digital Camera, Radiation Transmittance, and Laser Altimetry Methods. *Remote Sens. Environ.* **2000**, *74*, 45–57. [[CrossRef](#)]
17. Hu, Z.-Q.; He, F.-Q.; Yin, J.-Z.; Lu, X.; Tang, S.-L.; Wang, L.-L.; Li, X.-J. Estimation of Fractional Vegetation Cover Based on Digital Camera Survey Data and a Remote Sensing Model. *J. China Univ. Min. Technol.* **2007**, *17*, 116–120. [[CrossRef](#)]
18. Wu, D.; Wu, H.; Zhao, X.; Zhou, T.; Tang, B.; Zhao, W.; Jia, K. Evaluation of Spatiotemporal Variations of Global Fractional Vegetation Cover Based on GIMMS NDVI Data from 1982 to 2011. *Remote Sens.* **2014**, *6*, 4217–4239. [[CrossRef](#)]
19. Jiao, K.; Gao, J.; Liu, Z. Precipitation Drives the NDVI Distribution on the Tibetan Plateau While High Warming Rates May Intensify Its Ecological Droughts. *Remote Sens.* **2021**, *13*, 1305. [[CrossRef](#)]
20. Fan, J.; Xu, Y.; Ge, H.; Yang, W. Vegetation growth variation in relation to topography in Horqin Sandy Land. *Ecol. Indic.* **2020**, *113*, 106215. [[CrossRef](#)]
21. Zhan, Z.-Z.; Liu, H.-B.; Li, H.-M.; Wu, W.; Zhong, B. The Relationship between NDVI and Terrain Factors—A Case Study of Chongqing. *Procedia Environ. Sci.* **2012**, *12*, 765–771. [[CrossRef](#)]
22. Huang, C.; Yang, Q.; Guo, Y.; Zhang, Y.; Guo, L. The pattern, change and driven factors of vegetation cover in the Qin Mountains region. *Sci. Rep.* **2020**, *10*, 20591. [[CrossRef](#)] [[PubMed](#)]
23. Li, J.; Peng, S.; Li, Z. Detecting and attributing vegetation changes on China’s Loess Plateau. *Agric. For. Meteorol.* **2017**, *247*, 260–270. [[CrossRef](#)]
24. Wang, C.; Wang, J.; Naudiyal, N.; Wu, N.; Cui, X.; Wei, Y.; Chen, Q. Multiple effects of topographic factors on Spatio-temporal variations of vegetation patterns in the three parallel rivers region, Southeast Qinghai-Tibet Plateau. *Remote Sens.* **2021**, *14*, 151. [[CrossRef](#)]
25. Ren, Y.; Zhu, Y.; Baldan, D.; Fu, M.; Wang, B.; Li, J.; Chen, A. Optimizing livestock carrying capacity for wild ungulate-livestock coexistence in a Qinghai-Tibet Plateau grassland. *Sci. Rep.* **2021**, *11*, 3635. [[CrossRef](#)]
26. Fan, J.; Yu, H. Nature protection and human development in the Selincuo region: Conflict resolution. *Sci. Bull.* **2019**, *64*, 425–427. [[CrossRef](#)]
27. Gao, Q.-Z.; Wan, Y.-F.; Xu, H.-M.; Li, Y.; Jiangcun, W.-Z.; Borjigidai, A. Alpine grassland degradation index and its response to recent climate variability in Northern Tibet, China. *Quat. Int.* **2010**, *226*, 143–150. [[CrossRef](#)]
28. Yan, D.; Peng, S.; Ding, X.; Yu, Z. NDVI Variations and Its Responses to hydrothermal process in the Naqu River Basin, Qinghai-Tibet Plateau-Alpine Region. In Proceedings of the 7th International Conference on Energy Science and Chemical Engineering (ICESCE 2021), Dali, China, 21–23 May 2021; p. 01024.
29. Ma, C.; Xie, Y.; Duan, S.-B.; Qin, W.; Guo, Z.; Xi, G.; Zhang, X.; Bie, Q.; Duan, H.; He, L. Characterization of spatio-temporal patterns of grassland utilization intensity in the Selinco watershed of the Qinghai-Tibetan Plateau from 2001 to 2019 based on multisource remote sensing and artificial intelligence algorithms. *GIScience Remote Sens.* **2022**, *59*, 2217–2246. [[CrossRef](#)]
30. Ma, C.; Xie, Y.; Duan, H.; Wang, X.; Bie, Q.; Guo, Z.; He, L.; Qin, W. Spatial quantification method of grassland utilization intensity on the Qinghai-Tibetan Plateau: A case study on the Selinco basin. *J. Environ. Manag.* **2022**, *302*, 114073. [[CrossRef](#)]

31. Ge, J.; Meng, B.; Liang, T.; Feng, Q.; Gao, J.; Yang, S.; Huang, X.; Xie, H. Modeling alpine grassland cover based on MODIS data and support vector machine regression in the headwater region of the Huanghe River, China. *Remote Sens. Environ.* **2018**, *218*, 162–173. [[CrossRef](#)]
32. Martínez, B.; Gilabert, M.A. Vegetation dynamics from NDVI time series analysis using the wavelet transform. *Remote Sens. Environ.* **2009**, *113*, 1823–1842. [[CrossRef](#)]
33. Chen, T.; Niu, R.-Q.; Wang, Y.; Zhang, L.-P.; Du, B. Percentage of Vegetation Cover Change Monitoring in Wuhan Region Based on Remote Sensing. *Procedia Environ. Sci.* **2011**, *10*, 1466–1472. [[CrossRef](#)]
34. Liu, Y.; Li, L.; Chen, X.; Zhang, R.; Yang, J. Temporal-spatial variations and influencing factors of vegetation cover in Xinjiang from 1982 to 2013 based on GIMMS-NDVI3g. *Glob. Planet. Chang.* **2018**, *169*, 145–155. [[CrossRef](#)]
35. Liang, Y.; Zhang, Z.; Lu, L.; Cui, X.; Qian, J.; Zou, S.; Ma, X. Trend in Satellite-Observed Vegetation Cover and Its Drivers in the Gannan Plateau, Upper Reaches of the Yellow River, from 2000 to 2020. *Remote Sens.* **2022**, *14*, 3849. [[CrossRef](#)]
36. Kalisa, W.; Igbawua, T.; HENCHIRI, M.; Ali, S.; Zhang, S.; Bai, Y.; Zhang, J. Assessment of climate impact on vegetation dynamics over East Africa from 1982 to 2015. *Sci. Rep.* **2019**, *9*, 16865. [[CrossRef](#)]
37. Ndayisaba, F.; Guo, H.; Bao, A.; Guo, H.; Karamage, F.; Kayiranga, A. Understanding the Spatial Temporal Vegetation Dynamics in Rwanda. *Remote Sens.* **2016**, *8*, 129. [[CrossRef](#)]
38. Huang, C.; Yang, Q.; Huang, W.; Zhang, J.; Li, Y.; Yang, Y. Hydrological Response to Precipitation and Human Activities—A Case Study in the Zuli River Basin, China. *Int. J. Environ. Res. Public Health* **2018**, *15*, 2780. [[CrossRef](#)]
39. Zhang, X.-F.; Yan, H.-C.; Yue, Y.; Xu, Q.-X. Quantifying natural and anthropogenic impacts on runoff and sediment load: An investigation on the middle and lower reaches of the Jinsha River Basin. *J. Hydrol. Reg. Stud.* **2019**, *25*, 100617. [[CrossRef](#)]
40. Yao, H.; Shi, C.; Shao, W.; Bai, J.; Yang, H. Impacts of Climate Change and Human Activities on Runoff and Sediment Load of the Xiliugou Basin in the Upper Yellow River. *Adv. Meteorol.* **2015**, *2015*, 481713. [[CrossRef](#)]
41. Shi, H.; Hu, C.; Wang, Y.; Liu, C.; Li, H. Analyses of trends and causes for variations in runoff and sediment load of the Yellow River. *Int. J. Sediment Res.* **2017**, *32*, 171–179. [[CrossRef](#)]
42. Zhao, L.; Zou, D.; Hu, G.; Du, E.; Pang, Q.; Xiao, Y.; Li, R.; Sheng, Y.; Wu, X.; Sun, Z. Changing climate and the permafrost environment on the Qinghai–Tibet (Xizang) plateau. *Permafrost. Periglac. Process.* **2020**, *31*, 396–405. [[CrossRef](#)]
43. Kuang, X.; Jiao, J.J. Review on climate change on the Tibetan Plateau during the last half century. *J. Geophys. Res. Atmos.* **2016**, *121*, 3979–4007. [[CrossRef](#)]
44. Xu, H.-j.; Wang, X.-p.; Zhang, X.-x. Alpine grasslands response to climatic factors and anthropogenic activities on the Tibetan Plateau from 2000 to 2012. *Ecol. Eng.* **2016**, *92*, 251–259. [[CrossRef](#)]
45. Zhao, H.; Liu, S.; Dong, S.; Su, X.; Wang, X.; Wu, X.; Wu, L.; Zhang, X. Analysis of vegetation change associated with human disturbance using MODIS data on the rangelands of the Qinghai-Tibet Plateau. *Rangel. J.* **2015**, *37*, 77–87. [[CrossRef](#)]
46. Cai, H.; Yang, X.; Xu, X. Human-induced grassland degradation/restoration in the central Tibetan Plateau: The effects of ecological protection and restoration projects. *Ecol. Eng.* **2015**, *83*, 112–119. [[CrossRef](#)]
47. Jiao, C.; Yu, G.; He, N.; Ma, A.; Ge, J.; Hu, Z. Spatial pattern of grassland aboveground biomass and its environmental controls in the Eurasian steppe. *J. Geogr. Sci.* **2017**, *27*, 3–22. [[CrossRef](#)]
48. Gao, Q.; Wan, Y.; Li, Y.; Guo, Y.; Ganjurjav, Q.; Xiang, X.; Jiangcun, W.; Wang, B. Effects of topography and human activity on the net primary productivity (NPP) of alpine grassland in northern Tibet from 1981 to 2004. *Int. J. Remote Sens.* **2013**, *34*, 2057–2069. [[CrossRef](#)]
49. Lei, Y.; Zhu, Y.; Wang, B.; Yao, T.; Yang, K.; Zhang, X.; Zhai, J.; Ma, N. Extreme lake level changes on the Tibetan Plateau associated with the 2015/2016 El Niño. *Geophys. Res. Lett.* **2019**, *46*, 5889–5898. [[CrossRef](#)]
50. Huang, Y.; Xin, Z.; Dor-ji, T.; Wang, Y. Tibetan Plateau greening driven by warming-wetting climate change and ecological restoration in the 21st century. *Land Degrad. Dev.* **2022**, *33*, 2407–2422. [[CrossRef](#)]
51. Li, L.; Zhang, Y.; Wu, J.; Li, S.; Zhang, B.; Zu, J.; Zhang, H.; Ding, M.; Paudel, B. Increasing sensitivity of alpine grasslands to climate variability along an elevational gradient on the Qinghai-Tibet Plateau. *Sci. Total Environ.* **2019**, *678*, 21–29. [[CrossRef](#)]
52. Huang, K.; Zhang, Y.; Zhu, J.; Liu, Y.; Zu, J.; Zhang, J. The influences of climate change and human activities on vegetation dynamics in the Qinghai-Tibet Plateau. *Remote Sens.* **2016**, *8*, 876. [[CrossRef](#)]
53. Wang, X.; Yi, S.; Wu, Q.; Yang, K.; Ding, Y. The role of permafrost and soil water in distribution of alpine grassland and its NDVI dynamics on the Qinghai-Tibetan Plateau. *Glob. Planet. Chang.* **2016**, *147*, 40–53. [[CrossRef](#)]
54. Chen, J.; Yan, F.; Lu, Q. Spatiotemporal Variation of Vegetation on the Qinghai–Tibet Plateau and the Influence of Climatic Factors and Human Activities on Vegetation Trend (2000–2019). *Remote Sens.* **2020**, *12*, 3150. [[CrossRef](#)]
55. Peng, J.; Liu, Z.; Liu, Y.; Wu, J.; Han, Y. Trend analysis of vegetation dynamics in Qinghai–Tibet Plateau using Hurst Exponent. *Ecol. Indic.* **2012**, *14*, 28–39. [[CrossRef](#)]
56. Wang, Z.; Cui, G.; Liu, X.; Zheng, K.; Lu, Z.; Li, H.; Wang, G.; An, Z. Greening of the Qinghai–Tibet plateau and its response to climate variations along elevation gradients. *Remote Sens.* **2021**, *13*, 3712. [[CrossRef](#)]
57. Wang, R.; Wang, Y.; Yan, F. Vegetation Growth Status and Topographic Effects in Frozen Soil Regions on the Qinghai–Tibet Plateau. *Remote Sens.* **2022**, *14*, 4830. [[CrossRef](#)]
58. Soomro, A.G.; Babar, M.M.; Ashraf, A.; Memon, A. The relationship between precipitation and elevation of the watershed in the Khirthar national range. *Mehran Univ. Res. J. Eng. Technol.* **2019**, *38*, 1067–1076. [[CrossRef](#)]

59. Li, H.; Jiang, J.; Chen, B.; Li, Y.; Xu, Y.; Shen, W. Pattern of NDVI-based vegetation greening along an altitudinal gradient in the eastern Himalayas and its response to global warming. *Environ. Monit. Assess.* **2016**, *188*, 186. [[CrossRef](#)]
60. Zheng, K.; Wei, J.-Z.; Pei, J.-Y.; Cheng, H.; Zhang, X.-L.; Huang, F.-Q.; Li, F.-M.; Ye, J.-S. Impacts of climate change and human activities on grassland vegetation variation in the Chinese Loess Plateau. *Sci. Total Environ.* **2019**, *660*, 236–244. [[CrossRef](#)]
61. Li, X.; Gao, J.; Zhang, J. A topographic perspective on the distribution of degraded meadows and their changes on the Qinghai-Tibet Plateau, West China. *Land Degrad. Dev.* **2018**, *29*, 1574–1582. [[CrossRef](#)]
62. Silva, W.; Metzger, J.; Simões, S.; Simonetti, C. Relief influence on the spatial distribution of the Atlantic Forest cover on the Ibiúna Plateau, SP. *Braz. J. Biol.* **2007**, *67*, 403–411. [[CrossRef](#)] [[PubMed](#)]
63. Körner, C. The use of ‘altitude’ in ecological research. *Trends Ecol. Evol.* **2007**, *22*, 569–574. [[CrossRef](#)] [[PubMed](#)]
64. Fu, B.; Ouyang, Z.; Shi, P.; Fan, J.; Wang, X.; Zheng, H.; Zhao, W.; Wu, F. Current condition and protection strategies of Qinghai-Tibet Plateau ecological security barrier. *Bull. Chin. Acad. Sci.* **2021**, *36*, 1298–1306. (In Chinese) [[CrossRef](#)]
65. Zhou, H.; Yang, X.; Zhou, C.; Shao, X.; Shi, Z.; Li, H.; Su, H.; Qin, R.; Chang, T.; Hu, X. Alpine Grassland Degradation and Its Restoration in the Qinghai-Tibet Plateau. *Grasses* **2023**, *2*, 31–46. [[CrossRef](#)]
66. Zhang, H.; Chen, W.; Liu, W.; Liu, Z.; Liu, H. The evolution of settlement system and the paths of rural revitalization in alpine pastoral areas of the Qinghai-Tibet Plateau: A case study of Nagqu County. *Ecol. Indic.* **2023**, *150*, 110274. [[CrossRef](#)]
67. Dong, S.; Shang, Z.; Gao, J.; Boone, R.B. Enhancing sustainability of grassland ecosystems through ecological restoration and grazing management in an era of climate change on Qinghai-Tibetan Plateau. *Agric. Ecosyst. Environ.* **2020**, *287*, 106684. [[CrossRef](#)]

Disclaimer/Publisher’s Note: The statements, opinions and data contained in all publications are solely those of the individual author(s) and contributor(s) and not of MDPI and/or the editor(s). MDPI and/or the editor(s) disclaim responsibility for any injury to people or property resulting from any ideas, methods, instructions or products referred to in the content.